DOI 10.1007/s10946-024-10185-7
Journal of Russian Laser Research, Volume 45, Number 1, January, 2024

TEMPERATURE DEPENDENCE OF THE LINEWIDTHS AND AMPLITUDES OF THE SUB-DOPPLER RESONANCES OF ^{87}Rb D_2 LINE DETECTED WITH $\sigma(\sigma)$-POLARIZED PUMPING AND PROBE LASER BEAMS

Ersoy Şahin

TUBITAK National Metrology Institute (TUBITAK UME)
P.K. 54, Gebze 41470, Kocaeli, Turkey

E-mail: ersoy.sahin @ tubitak.gov.tr

Abstract

We asses impact of the temperature of ^{87}Rb atoms on the linewidths and amplitudes of the F = 1 → F′ = 0, 1, 2 and F = 2 → F′ = 1, 2, 3 hyperfine resonances of the ^{87}Rb D_2 line, using the circularly-polarized pumping beam and the probe laser beam. To achieve high-precision and accuracy, frequency-stabilized narrow-linewidth extended-cavity diode lasers, we employ a temperature-controlled Fabry–Pérot interferometer and a magnetically-shielded temperature-controlled Rb cell with dimensions in the centimeter range, containing enriched ^{87}Rb atoms. Consequently, the linewidth and amplitude measurements are conducted with inaccuracies of 1.5 MHz and 0.4 mV, respectively.

Keywords: hyperfine resonances of ^{87}Rb D_2 line, linewidth, amplitude, polarization.

1. Introduction

Diode lasers play a crucial role in atomic frequency standards, magnetometers, and wavelength standards, thanks to their frequency stabilization achieved through sub-Doppler absorption resonances of ^{87}Rb atoms [1–6]. These resonances are identified within the Doppler broadening of the linewidth, a consequence of atoms interacting with counter-propagating pumping and probe laser beams derived from a single-frequency laser source [7, 8]. In the process of frequency stabilization, the derivative of the resonances, extracted through frequency modulation techniques applied to saturation absorption resonances, serves as a feedback signal for the piezoelectric transducer (PZT) or the current of the diode lasers. The attainable level of frequency stability for the laser depends on the discriminator slope of the feedback signal, which is determined by the ratio of the resonance amplitude to the width of the resonant line [9]. Various methods, including the frequency-modulation (FM) spectroscopy [10], dichroic atomic laser lock (DAVLL) [11], velocity-selective saturated-absorption spectroscopy [12], polarization spectroscopy [13,14], and Zeeman modulation technique [15] are employed to derive the resonance derivatives. In the FM modulation technique, linearly-polarized pumping and probe laser beams are utilized for the generation and detection of saturation resonances, while circular polarizations are employed in other techniques.

The linewidth and amplitude of resonances are intricately linked to the optical anisotropy of the atomic medium, as expressed by the electric susceptibility, which depends on both the polarization of the pumping and probe laser beams and the ambient temperature of the atoms [16]. While measurements of the linewidth and amplitude of the hyperfine resonances of the ^{87}Rb D_2 line are lacking, theoretical

Manuscript submitted by the author in English on December 11, 2023.

and analytical studies have focused on impact of the polarization of the pumping and probe laser beams on the spectra of resonances and amplitudes [16–18]. The resonance amplitudes for the ^{87}Rb line were theoretically evaluated in [16], analyzed in [17], and calculated for F $= 1 \rightarrow$ F$' = 0$, 1, 2 and F $= 2 \rightarrow$ F$' = 1$, 2, 3 hyperfine resonances of the ^{87}Rb D_2 line in [18]. In a prior study, the influence of temperature on the linewidth and amplitudes of hyperfine resonances of the ^{87}Rb D_2 line F $= 1 \rightarrow$ F$' = 0$, 1, 2 and F $= 2 \rightarrow$ F$' = 1$, 2, 3 and crossovers (CO) were measured, using linearly-polarized pumping and probe laser beams [19]. In this study, we detect the hyperfine resonances of the ^{87}Rb D_2 line and measure, using circularly-polarized pumping and probe laser beams.

2. Linewidth and Amplitude Measurements of the Hyperfine Resonances of ^{87}Rb D_2 Line

The measurements are conducted using the experimental setup shown in Fig. 1. We employ frequency-stabilized narrow-linewidth extended-cavity diode lasers (ECDLs), as the reference L_{ref} and recording L_{rec} lasers, respectively. The hyperfine resonances of the ^{87}Rb line are ecorded by scanning the frequency of the L_{rec} laser, while the frequency scale of the measurements is established, using L_{ref}, through the detection of the beat frequency between the lasers. To ensure the stability of the ECDLs, we utilize the third derivative of the hyperfine resonances of ^{87}Rb atoms and the first derivative of the transmission resonances of a temperature-controlled Fabry–Pérot interferometer (TFPI). The L_{ref} laser is stabilized to the hyperfine resonances of ^{87}Rb atoms, while the stabilization of L_{rec} is achieved with respect to the transmission resonances of TFPI. As the modulation frequency, employed for obtaining derivatives of hyperfine resonances, increases the linewidths of the resonances and induces fluctuations in their ampli-

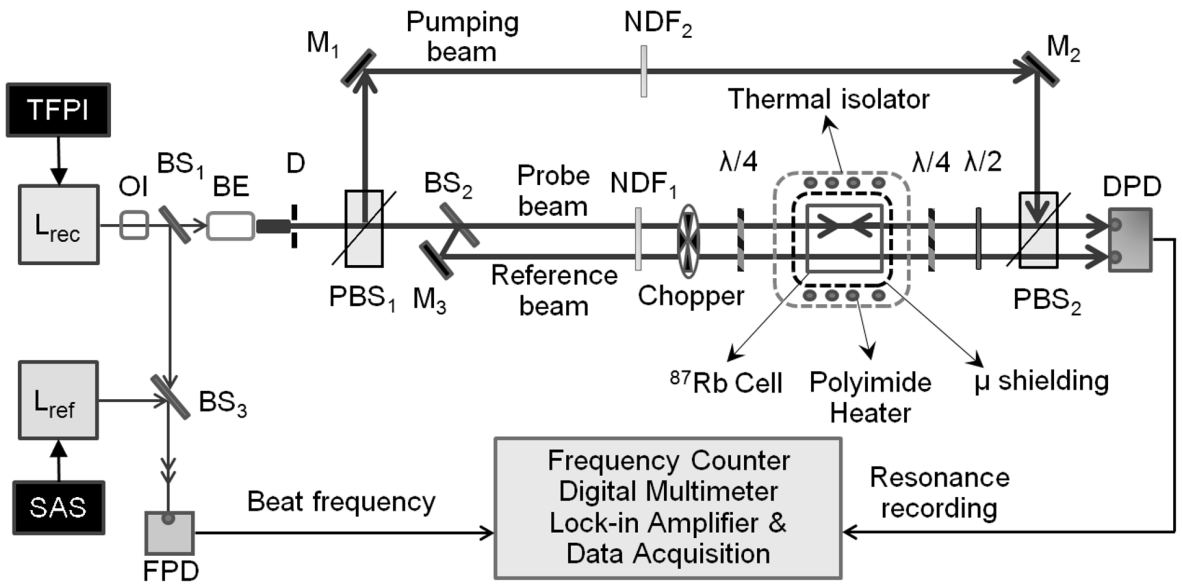

Fig. 1. Measurement setup. Recording Laser (L_{rec}), temperature-controlled Fabry–Pérot interferometer (TFPI), optical isolator (OI), beam splitter (BS), beam expander (BE), diaphragm (D), polarizing beam splitter (PBS), mirror (M), neutral density filter (NDF), differential photodetector (DFD), fast photodetector (FPD), reference laser (L_{ref}), and saturated absorption spectroscope (SAS).

tudes, neither the piezoelectric transducer (PZT) nor the current of L_{rec} is modulated. The modulation signal is applied to the PZT of TFPI, and the feedback signal is applied to the PZT of the L_{rec} laser for frequency stabilization. The frequency of L_{rec} is scanned by applying a ramp signal to the PZT of TFPI. The measurements are conducted, using a magnetically-shielded, temperature-controlled enriched ^{87}Rb cell, with dimensions of 5 cm in length and 3 cm in diameter. The resonances are detected, using circularly-polarized, counter-propagating pumping and probe laser beams, with diameters of 3 mm. The half-wave plate is used to adjust the angle of the pumping-beam polarization, which is 90° different linear polarization according to the probe, and to generate the probe and pumping laser beams with parallel linear polarizations. The quarter-wave plate $\lambda/4$, placed after the half-wave plate, is used to convert the polarization of the pumping beam from the linear polarization to the circular polarization. For linewidth and amplitude measurements of $F = 1 \rightarrow F' = 0, 1, 2$ and crossover resonances, the power of the pumping beam is set at 205 μW (2.9 mW/cm^2), while for $F = 2 \rightarrow F' = 1, 2, 3$, it is set at 250 μW (3.54 mW/cm^2), and the probe beam power is maintained at 10 μW (0.14 mW/cm^2). We carry out the registration of the resonances, using a chopper, computer-controlled lock-in amplifier, digital voltmeter, and frequency counter. This approach facilitates precise and accurate measurements.

The effect of the ^{87}Rb atomic gas temperature on $F = 1 \rightarrow F' = 0, 1, 2$, $F = 1 \rightarrow F' = 1, 2, 3$, and crossover resonances are presented in Fig. 2. The resonances are recorded by scanning the temperature of the Rb cell, ranging from 22.5°C to 57.5°C for $F = 1 \rightarrow F' = 0, 1, 2$ resonances, and from 22.5°C to 52.5°C for $F = 2 \rightarrow F' = 1, 2, 3$ resonances. As shown in Fig. 2, dispersive line shapes in the $F = 2 \rightarrow F' = 3$ resonance are observed, being attributed to the light pressure induced by the pump

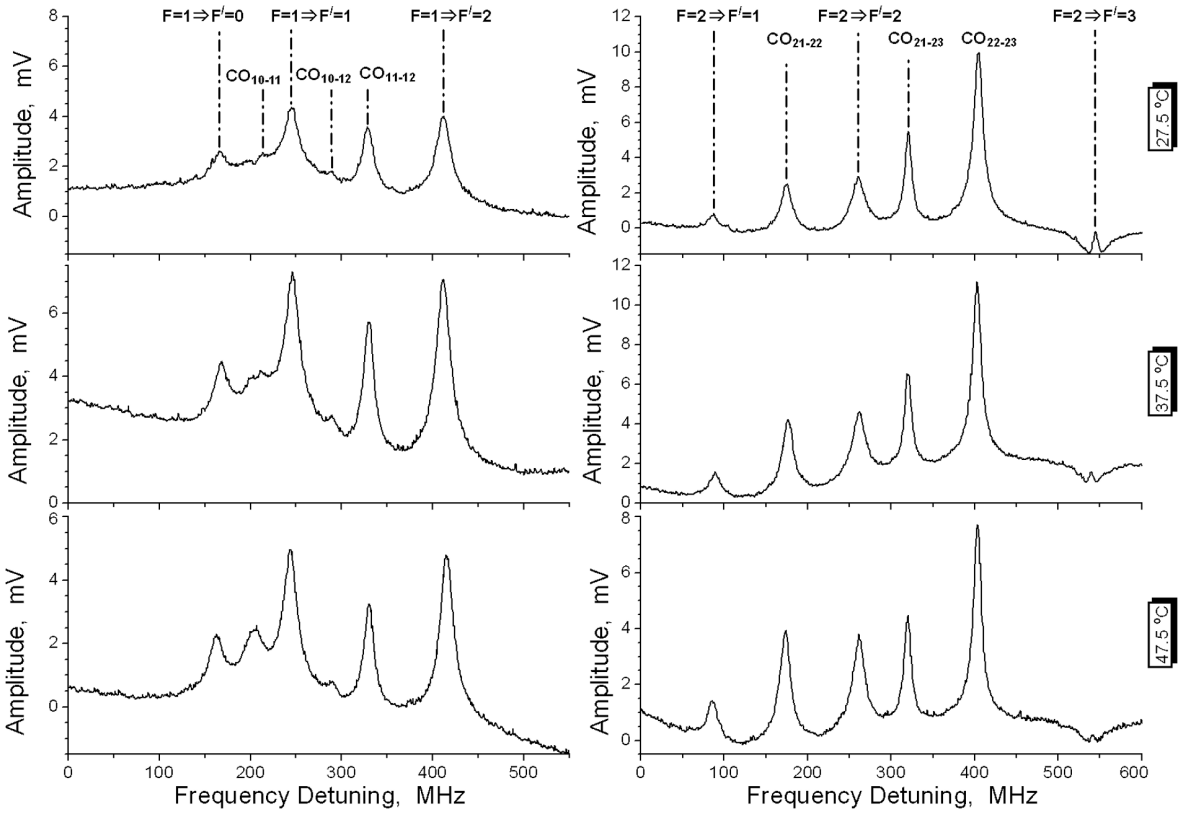

Fig. 2. The effect of the ^{87}Rb atomic gas temperature on $F = 1 \rightarrow F' = 0, 1, 2$, $F = 2 \rightarrow F' = 1, 2, 3$, and crossover resonances.

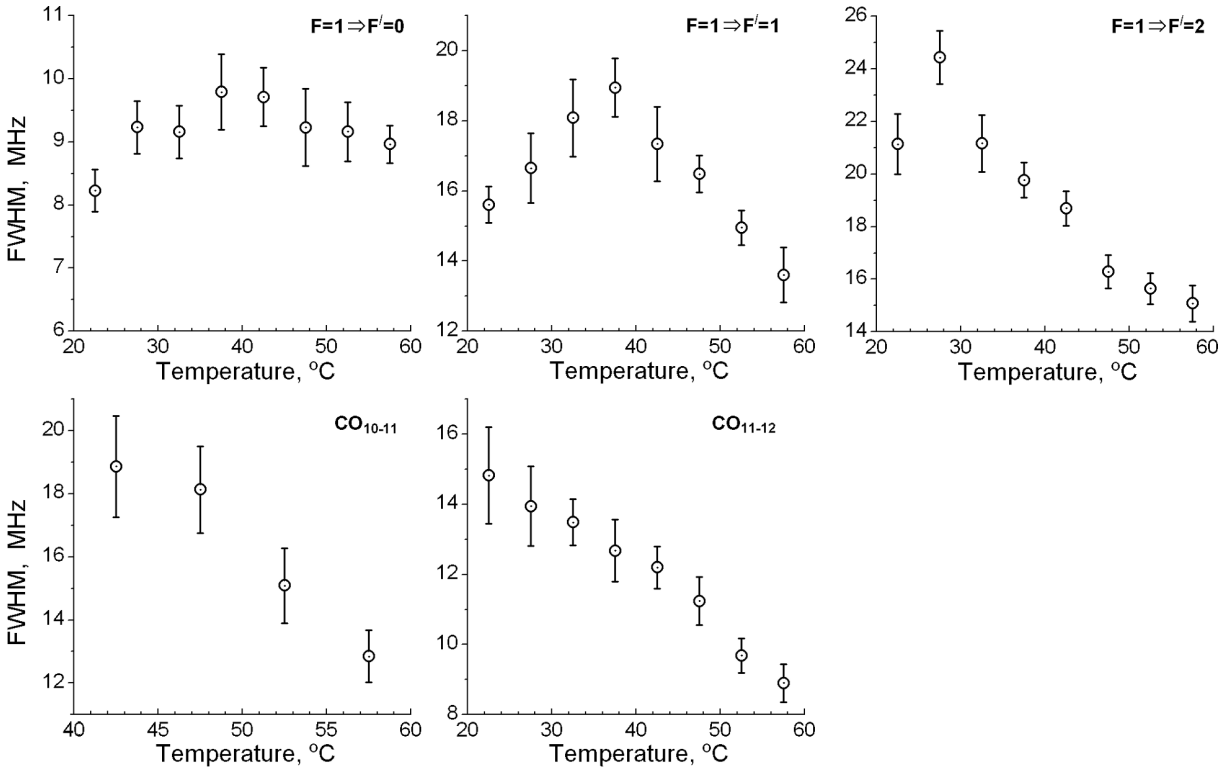

Fig. 3. The effect of the ^{87}Rb atomic gas temperature on the linewidth of F = 1 → F′ = 0, 1, 2, CO_{10-11}, and CO_{10-12} resonances.

laser beam [17].

In Figs. 3 and 4, we show impacts of the ^{87}Rb atomic gas temperature on the linewidth and amplitude of F = 1 → F′ = 0, 1, 2 and the crossover resonances. Due to insufficient amplitude, we exclude the CO_{10-12} resonance from the analysis, and its temperature-dependent effects are not presented in Figs. 3 and 4. As the temperature increases, the linewidths of the resonances widened up to 37.5°C for F = 1 → F′ = 0 and F = 1 → F′ = 1, and up to 27.5°C for F = 1 → F′ = 2. A narrowing trend is observed in temperature above these values. In contrast, the linewidths of crossover resonances, CO_{10-11} and CO_{11-12}, display a linear decrease; see Fig. 3. The measurements indicate that the maximum values of amplitudes for F = 1 → F′ = 0, 1, 2 and crossover resonances are connected with increase in the temperature up to 42.5°C, after which a decrease is observed; see Fig. 4. We identify the CO_{10-11} crossover resonance above 40°C; consequently, we conduct the analysis of linewidth and amplitude for this resonance above 40°C.

The changes in linewidths and amplitudes of F = 2 → F′ = 1, 2, 3 and crossover resonances with the temperature of the ^{87}Rb atomic gas are shown in Figs. 5 and 6. One observes that the linewidths of the resonances narrow with increase in the temperature, except for the CO_{21-23} resonance shown in Fig. 5. There is no noticeable change in the amplitudes of the F = 2 → F′ = 2, CO_{21-23}, and CO_{22-23} resonances, in the temperature range of 22.5°C to 37.5°C. However, the amplitudes linearly decrease, when the temperature of the ^{87}Rb atomic gas exceeds 37.5°C. We observe a linear increase in the amplitude with temperature for the F = 2 → F′ = 1 resonance, while a decrease is noted for the F = 2 → F′ = 3 resonance. The largest amplitude values for the CO_{21-22} and CO_{21-23} resonances are

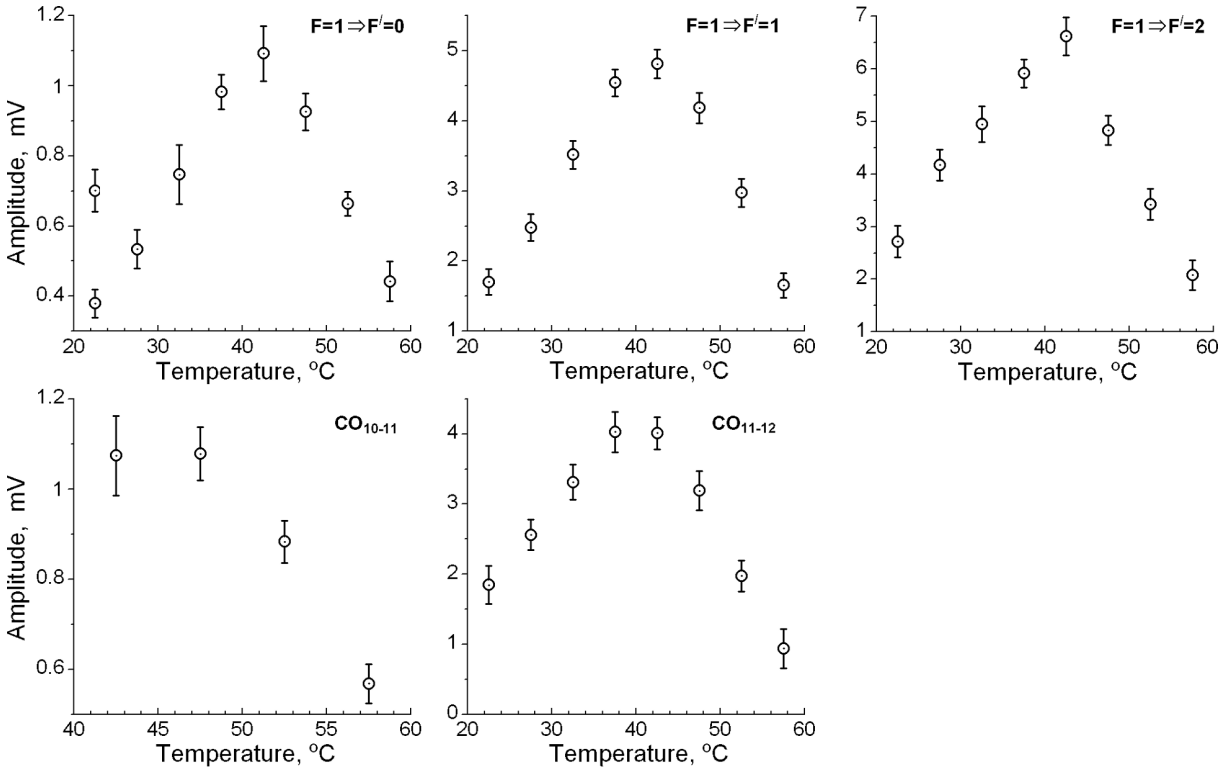

Fig. 4. The effect of the ^{87}Rb atomic gas temperature on the amplitude of F = 1 → F′ = 0, 1, 2, CO_{10-11}, and CO_{10-12} resonances.

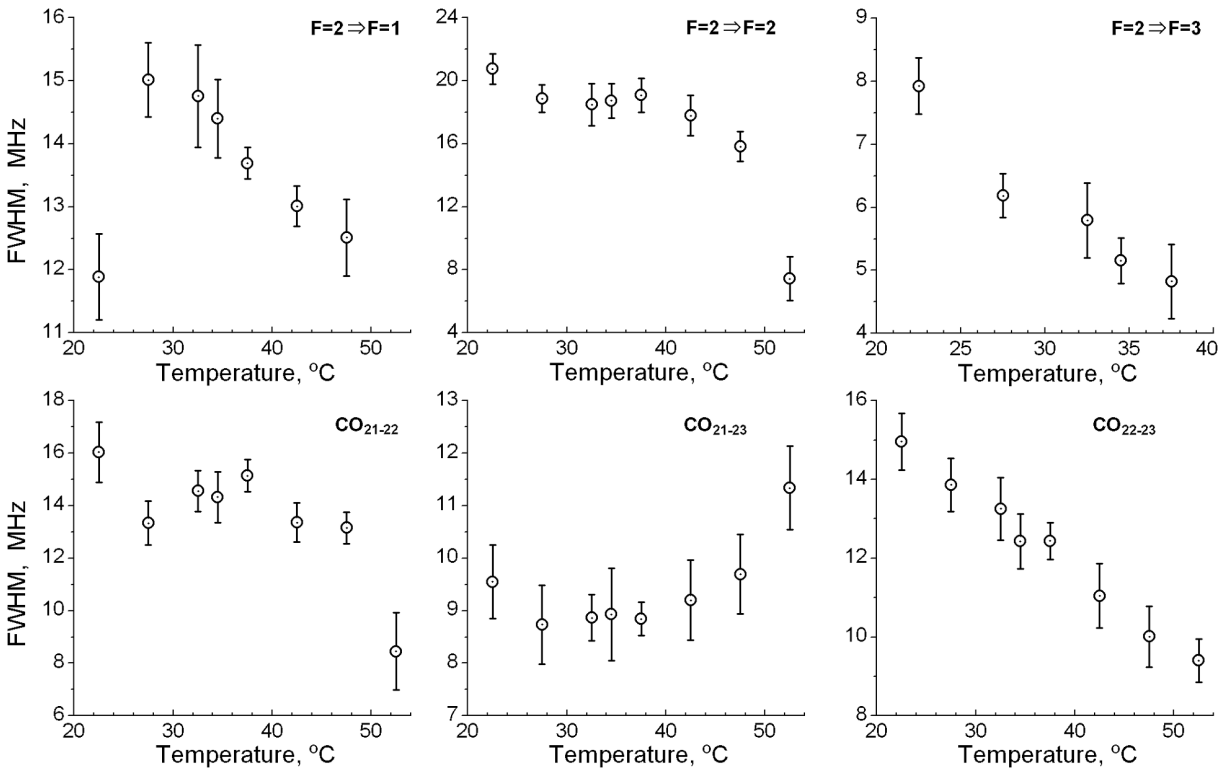

Fig. 5. The effect of the ^{87}Rb atomic gas temperature on the linewidth of F = 2 → F′ = 1, 2, 3, CO_{21-22}, $CO_{21-23,}$, and CO_{22-23} resonances.

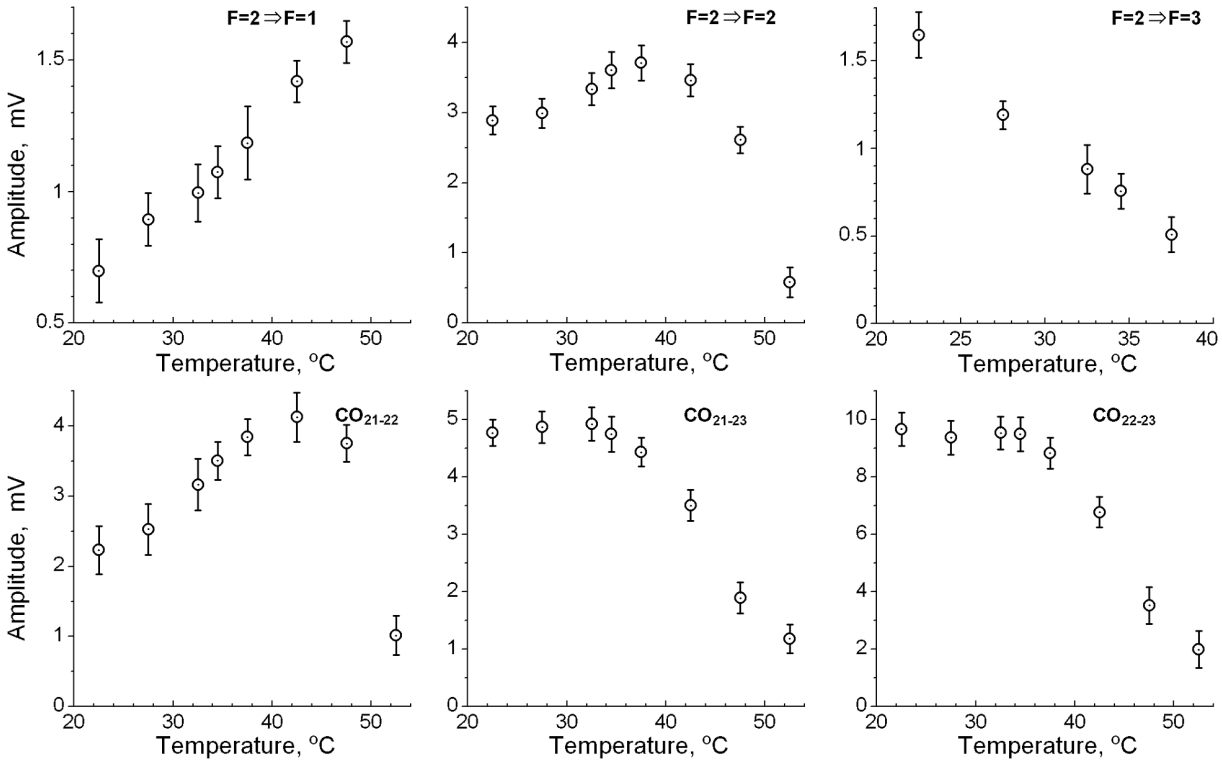

Fig. 6. The effect of the ^{87}Rb atomic gas temperature on the amplitude of F = 2 → F′ = 1, 2, 3, CO_{21-22}, $CO_{21-23,}$, and CO_{22-23} resonances.

almost twice those of the largest amplitudes for F = 2 → F′ = 1 and F = 2 → F′ = 2, respectively, whereas the amplitude of CO_{22-23} is five times that of F = 2 → F′ = 3; see Fig. 6.

We derive the resonant linewidth and amplitude values presented in the graphs by averaging the data obtained from five consecutive measurements. The error bars indicate uncertainties of smaller than 1.5 MHz for the linewidth measurements and 0.4 mV, for the amplitude measurements. To detect and measure all sub-Doppler resonances of ^{87}Rb atoms, we deliberately maintain the laser intensity higher than necessary. The saturate-broadened linewidth is calculated as $\Gamma' = \Gamma[(1 + (I/I_{\rm Sat})]^{1/2}$, where I is the intensity of the laser beam, and $I_{\rm Sat}$ is the saturation intensity [7]. Saturation line broadenings are calculated as 2.5 MHz for F = 2 → F′ = 1, 2, 3 resonances and 2.1 MHz for F = 1 → F′ = 0, 1, 2 resonances, utilizing the laser intensities employed in the measurements. In the calculations, we use $I_{\rm Sat} = 3.58$ mW/cm^2, a value specified for circularly polarized pumping and probe laser beams. In Figs. 3 and 5, we observe the linewidths commence at 8 MHz rather than 6 MHz for F = 1 → F′ = 0 and F = 2 → F′ = 3.

3. Conclusions

In this study, we meticulously examined the impact of temperature variations on the linewidth and amplitude measurements of hyperfine resonances within the ^{87}Rb D_2 line. Notably, we observed that the linewidths of the F = 1 → F′ = 0, 1, 2 resonances exhibited a broadening trend up to a certain tempera-

ture threshold, followed by a subsequent narrowing effect, and the linewidths of the crossover resonances demonstrated a linear decrease. On the other hand, the amplitudes of these resonances decreased with increasing temperature after reaching their maximum values. Furthermore, the measurements unveiled a distinct behavior in the linewidth of $F = 2 \rightarrow F' = 1, 2, 3$ and crossover resonances. A narrowing trend was observed with temperature, with the exception of the CO_{21-23} resonance. Interestingly, the largest amplitudes of the CO_{21-22} and CO_{21-23} resonances were nearly doubled compared to the $F = 2 \rightarrow F' = 1$ and $F = 2 \rightarrow F' = 2$ resonances, respectively. Moreover, the largest amplitude of CO_{22-23} surpassed that of $F = 2 \rightarrow F' = 3$ by a factor of five.

In summary, our findings provide insight into the complex interaction between temperature variations and the hyperfine resonances of the ^{87}Rb D_2 line. These observations offer valuable understanding of the behavior of linewidths and amplitudes under varying thermal conditions.

References

1. Y. Ovchinnikov and M. Giuseppe, *Metrologia*, **48**, 3 (2011).
2. J. Vanier, *Appl. Phys. B*, **81**, 421 (2005).
3. G. S. Pati, R. Tripathi, R. S. Grewal, et al., *Phys. Rev. A*, **104**, 033116 (2021).
4. T. J. Quinn, *Metrologia*, **40**, 2 (2003).
5. J. D. Elgin, T. P. Heavner, J. Kitching, et al., *Appl. Phys. Lett.*, **115**, 033503 (2019).
6. S. Micalizio, F. Levi, C. E. Calosso, et al., *GPS Solut.*, **25**, 94 (2021).
7. D. A. Smith and I. G. Hughes, *Am. J. Phys.*, **72**, 631 (2004).
8. M. Himsworth and T. Freegarde, *Phys. Rev.*, **81**, 023423 (2010).
9. G. Mileti and P. Thomann, "Study of the S/N Performance of Passive Atomic Clocks Using a Laser Pumped Vapour," in: *Proceedings of the 9th European Frequency and Time Forum*, Societé Française des Microtechniques et de Chronométrie, Besançon (1995), pp. 271–276.
10. G. C. Bjorklund, M. D. Levenson, W. Lenth, and C. Ortiz, *Appl. Phys.*, **32**, 145 (1983).
11. S. Pustelny, V. Schultze, and D. Budker, *Rev. Sci. Instrum.*, **87**, 063107 (2016).
12. S. Chakrabarti, B. Ray, and P. N. Ghosh, *Eur. Phys. J. D*, **42**, 359 (2007).
13. M. L. Harris, C. S. Adams, S. L. Cornish, et al., *Phys. Rev. A*, **73**, 062509 (2006).
14. C. Wieman and T. W. Hänsch, *Phys. Rev. Lett.*, **36**, 1170 (1976).
15. E. Sahin, *Appl. Phys. B*, **127**, 148 (2021).
16. S. Nakayama, *Jpn. J. Appl. Phys.*, **24**, 1R (1985).
17. G. Moon and H. R. Noh, *J. Opt. Soc. Ame. B*, **25**, 5, (2010).
18. H.-R. Noh, *J. Korean Phys. Soc.*, **57**, 6 (2010).
19. E. Sahin, *Eur. Phys. J. D*, **76**, 119 (2022).